

Assessment of the Reactivity Effects of Gas Cooled Fast Reactor

J. Luley¹, B. Vrban¹, Š. Čerba¹, J. Haščík¹

¹Slovak University of Technology in Bratislava (STU), Bratislava, Slovakia

E-mail contact of main author: jakub.luley@stuba.sk

Abstract. Presented paper assess standard reactivity effects, as coolant void effect and Doppler effect, of the power scale Gas cooled Fast Reactor (GFR 2400) in a comprehensive manner by application of the perturbation theory. To achieve high validity of the results the conventional SCALE 6 system and adapted computational scheme (ACS) are utilized. The ACS is based on standard computational package incorporating codes like TRANSX, PARTISN, DIF3D, PORK and STUUP with cross section data library optimized for fast reactor applications. The reactivity effects of the GFR 2400 core were calculated in a range of the pre-defined temperatures and coolant pressures. Coolant void effect for nominal and lowest operational pressure and Doppler effects for highest temperature increase and decrease were identified as most important reactivity effects. Spatial distribution of the selected reactivity effects is analyzed and presented in this paper for further evaluation. In the next step, sensitivity and uncertainty analysis is performed for these reactivity effects where the sensitivity coefficients are validated via direct perturbation calculation and comparison of energy profiles. In case of possible optimization of selected reactivity effects, the most sensitive isotopes and contributors to the overall uncertainty are identified. The final part of the paper is dedicated to the first optimization studies and preliminary results are presented. Two possible options of optimizations are proposed; homogeneous and heterogeneous. In the heterogeneous case the rod follower volume is used for application of materials which can possibly influence the reactivity effects. In the second case the core design modifications are homogeneously distributed over the entire core volume. Finally, in the conclusion recommendations and some drawbacks are given for further analyses.

Key Words: Gas cooled Fast Reactor, coolant void effect, Doppler Effect, sensitivity analysis

1. Introduction

One of the main challenges, and also potential advantage, in terms of implementation of GEN IV innovative technologies in the nuclear fuel cycle is their safety. The GFR 2400 reactor is considered as a conceptual design of the large scale GEN IV Gas-Cooled Fast Reactor. It features ceramic fuel, composite SiC-SiC_{fib} cladding with refractory liners and helium coolant, being expected to be operated at relatively high temperatures and power densities. Due also to low thermal inertia of helium, the temperature changes during transients are very fast. This is raising demand for highly reliable and efficient safety systems and it could also lead to power oscillations [1]. Since GFR 2400 lacks any experimental data, the questions related to its safety are more complex and the assessment of its performance could be made only based on computational experience. Static neutron transport calculation is the first step to identify crucial integral parameters. In many cases, these information are not sufficient and therefore scientists could benefit from application of the Perturbation Theory in post-processing stage to investigate local effects related to specific initiation events. Within the reactor analysis and design calculation, reactivity decomposition, sensitivity and uncertainty analysis offers to a nuclear engineer a unique insight into the investigated system. Estimation of the change of the system response (k_{eff} , reactivity effect), due to change in some input parameter, can identify important processes and evaluate the influence of variation in this

parameter. Decomposition of the response change to reactions, individual nuclides and spatial components establish multipurpose database effectively applicable in reactor system analysis and design development. The base equation of the Perturbation Theory can be written in a simple form as follows:

$$\Delta k \cong \frac{\langle \Phi^* \left(\frac{1}{k} \frac{\partial P}{\partial \Sigma} - \frac{\partial L}{\partial \Sigma} \right) \Phi \rangle}{\langle \Phi^* P \Phi \rangle}, \quad (1)$$

where Δk is the k_{eff} change with respect to Σ as a macroscopic cross section. Therefore $\partial \Sigma$ represents the change in nuclear data, like cross sections, fission spectrum and nubar, or atom density. Symbols L and P in Eq. (1) are net loss and production Boltzman operators; Φ^* and Φ are adjoint and forward neutron fluxes respectively. All input information necessary to determine the k_{eff} change by Eq. (1) can completely characterize the investigated system, therefore the sensitivity coefficients can be considered as a unique fingerprint of the system [2].

2. GFR 2400 Core and Computational System Characterization

2.1. GFR 2400 Core Characterization

The GFR 2400 reactor design is a large scale power unit with thermal power of 2400 MW_{th}. This fast-spectrum reactor is a helium-cooled system and it works with a closed fuel cycle. In order to ensure adequate heat transfer, primary coolant pressure during normal operation reaches 7 MPa. The internal components of GFR 2400 core need to withstand high temperatures, therefore ceramic compositions are under investigation as a promising solution for the used materials. The 3D hexagonal models of GFR 2400 MW_{th} core were prepared on the basis of the carbide fuel pin type core design developed by CEA. The core model is composed of inner and outer heterogeneously modelled fuel regions with different Pu contents. The inner part consists of 264 and the outer part of 252 fuel assemblies. The control rod system is composed of 13 DSDs and 18 CSDs with the same material composition of B₄C (90% of ¹⁰B). The rod follower is made of a structural material (containing SiC) which was also implemented into this model. [3]

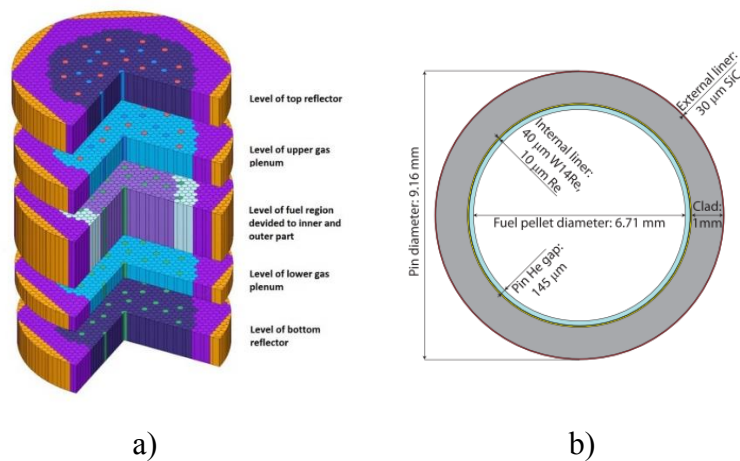


FIG. 1. Cross section of the GFR 2400 core (a) and fuel pin (b) [3].

The initial core calculation refers to the state where all control rod assemblies are positioned above the top edge of the fuel part. The core fuel region is surrounded by six rings of Zr₃Si₂ reflector assemblies. The 3D cross-sectional view of the GFR 2400 core model is shown in

FIG. 1 *Error! Reference source not found.*-a. Fuel pins were defined as a fuel pellet made of UPuC with a volumetric content of PuC in the inner core (IC) is 14.2%, and 17.6% in the outer core (OC). The isotopic composition of uranium corresponds to natural uranium, whereas plutonium is composed of twice recycled mixed oxide (MOX) fuel available in France since 2016. The fuel cladding is composed of silicon-carbide in combination with tungsten and tungsten-rhenium liners (see FIG. 1-b.) [3].

2.2. Computational System Characterization

Perturbation calculation was based on the developed code PORK, which is able to read standard CCCC interface files [4] including problem dependent multigroup cross section library in ISOTXS format. Forward and adjoint flux calculation was carried out using diffusion code DIF3D [5] and KAFAX-E70 [6] library, based ENDF/B-VII evaluated data. For validation purposes the sensitivity coefficients were calculated also by the utilities from SCALE system [7]. TSUNAMI-3D code was employed in sensitivity analyses of k_{eff} and TSAR code in sensitivity analyses of chosen reactivity effects. Forward and adjoint transport calculations were carried out with KENO6 based on ENDF/B-VII 238 group nuclear data library. The resonance self-shielding calculation was performed due to the multi-group cross section data used in both computational routes. SCALE system is capable to perform only cell calculation at the level of fuel pin with definition of cladding and coolant in an infinite lattice, where the spectral calculation was done using CENTRUM code. Methods used in the multi-group cross sections processing procedures for DIF3D calculations allow us consider resonance self-shielding effect as well as the spatial boundary effects. In this case, two level of cross section calculation was necessary to perform, where in the second level the cross sections were condensed from 150 to 25 groups structure by using zone averaged neutron flux from RZ transport calculation. In the case of evaluation of the uncertainties of integral system response induced by the cross sections, two cross section covariance libraries were used. Within SCALE calculations standard 44GROUPCOV library was used. The library includes evaluated covariances obtained from ENDF/B-VII.0, ENDF/B-VI, and JENDL-3.3 for more than 50 materials [7]. For computational route based on PORK code (see FIG. 2), cross section covariance library was prepared, in accordance with used 25 group energy structure, using ENDF/B-VII.1 and JENDL-4.0 evaluated data. Covariance data for 44 nuclides from material composition of GFR 2400 core were used. Subsequently, the responses uncertainties were calculated utilizing the in-house code STUUP.

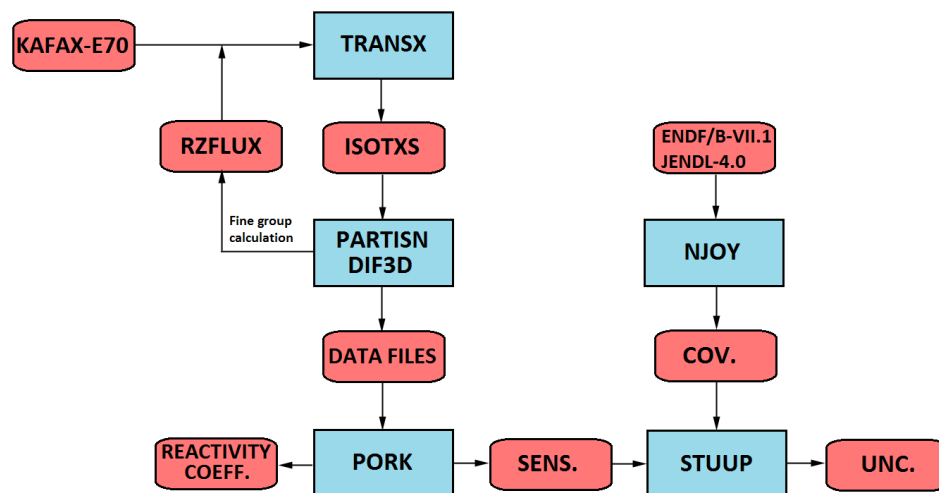


FIG. 2. Computational scheme for PORK code.

3. Discussion and Results

To determine reactivity effects based on the Doppler Effect and core voiding the several combinations of the possible temperatures and depressurization fractions were employed to the core model. Limitation factors of the normal and off-normal operation states are the melting point of the fuel, the loss of coolant pressure, the zero power temperature or the cold case. Coolant depressurization is considered only in the fuel region from 7 MPa to 1 MPa ($\Delta\rho_{7 \rightarrow 1}$), which according to the design should be the lowest pressure providing decay heat removal by natural circulation. Temperatures of the fuel and coolant were selected in the range of 453-2063 K where some combinations can be considered as unlikely in predictable reactor operation. These reactivity effects are presented in the following tables giving the complex description of investigated system and were calculated based on Eq. (2).

$$\Delta\rho_{xy} = \rho_y - \rho_x = \frac{k_y - k_x}{k_y k_x}. \quad (2)$$

In Eq. (2), ρ is the reactivity excess corresponding to the effective multiplication coefficient of x, y reactor core state.

In Table I and II are presented results with two type of uncertainties. In the case of reactivity effects determined by the DIF3D code, all calculated uncertainties are induced by nuclear data uncertainties. In the case of SCALE system, all uncertainties come from statistical character of the Monte Carlo method. Only highlighted SCALE uncertainties are induced by nuclear data uncertainties. In both cases the cross section uncertainty ΔR was evaluated by the well-known sandwich formula:

$$\Delta R^2 = S_R U S_R^T \quad (3)$$

where the symbol S denotes the cross section sensitivity coefficients and U is the associated covariance matrix.

TABLE I: REACTIVITY EFFECTS FOR DEFINED FUEL TEMPERATURES.

Temperature of fuel [K]	$\Delta\rho_{7 \rightarrow 1}$ [pcm]		$\Delta\rho_{T_{\text{fuel}}}$ [pcm]	
	DIF3D	SCALE	DIF3D	SCALE
453	212.9 \pm 10.3	196.7 \pm 13.0	1183.1 \pm 36.9	1086.21 \pm 67.9
663	219.5 \pm 10.5	219.0 \pm 13.1	708.8 \pm 21.5	699.8 \pm 13.2
913	222.2 \pm 10.5	188.0 \pm 13.1	342.9 \pm 10.2	370.2 \pm 13.2
1263	226.0 \pm 10.6	213.8 \pm 86.7	0.0 \pm 0.0	0.0 \pm 13.3
1663	229.4 \pm 10.7	219.8 \pm 13.3	-282.9 \pm 8.1	-290.6 \pm 13.3
2063	232.0 \pm 10.8	224.1 \pm 13.2	-503.7 \pm 14.3	-523.1 \pm 92.5

The reactivity effects of coolant pressure change ($\Delta\rho_{7 \rightarrow 1}$) and fuel temperature change ($\Delta\rho_{T_{\text{fuel}}}$) depending on the fuel temperature are presented in Table I for reference design of the GFR 2400. According to the results, void reactivity effect of the core is almost insensitive to a fuel temperature. Small increase towards to higher temperatures can be seen but 9 % increases within 1600 K change may be considered as a negligible. Reactivity effects of fuel temperature change are consistent with published research [3]. Small overestimation of reactivity effect due to temperature change to 453 K can be seen in case of DIF3D code. The source of difference can be explained by the statistical fluctuations of Monte Carlo

calculations or influence of a temperature interpolation during cross section data processing (453 K lies almost in the middle between 300 K and 600 K for which the data are stored in libraries) in combination with logarithmic dependence of Doppler coefficient. Uncertainties were determined by the STUUP code reach about 3 % for fuel temperature change and around 5 % for void reactivity effects which is far below GIF recommendations [3]. In the case of SCALE system, the uncertainties vary between 6 % to 40 %. The main contributors to total uncertainty are elastic scattering of ^{90}Zr and inelastic scattering of ^{238}U . Noticeable difference between STUUP and SCALE uncertainties is based on the covariance matrices improvement in ENDF/B-VII.1 and JENDL-4.0 library compared to ENDF/B-VII.0. Some contribution to the obtained differences is also driven by the statistical uncertainty of the sensitivity coefficients.

TABLE II: REACTIVITY EFFECTS FOR DEFINED COOLANT TEMPERATURES.

Temperature of coolant[K]	$\Delta\rho_{7 \rightarrow 1}$ [pcm]		$\Delta\rho_{\text{Tcoolant}}$ [pcm]	
	DIF3D	SCALE	DIF3D	SCALE
453	448.7 \pm 21.1	456.0 \pm 32.9	-261.7 \pm 12.3	-251.4 \pm 73.9
663	308.9 \pm 14.5	301.4 \pm 13.2	-97.9 \pm 4.6	-90.3 \pm 13.3
913	226.0 \pm 10.6	213.8 \pm 86.7	0.0 \pm 0.0	0.0 \pm 0.0
1263	163.4 \pm 7.7	197.6 \pm 13.3	72.4 \pm 3.4	57.5 \pm 13.3
1663	124.3 \pm 5.8	110.3 \pm 13.3	118.2 \pm 5.6	110.8 \pm 13.3
2063	100.3 \pm 4.7	105.7 \pm 13.3	146.2 \pm 6.9	146.2 \pm 13.3

The reactivity effects of coolant density change due to change in pressure ($\Delta\rho_{7 \rightarrow 1}$) and temperature ($\Delta\rho_{\text{Tcoolant}}$) are presented in Table II. Strong influence of void reactivity effect on coolant temperature can be seen. While absolute value of reactivity effects is relatively small, approaching the temperature 453 K void reactivity effect exceeds effective delayed neutron fraction, determined by PORK to $\beta_{\text{eff}} = 377 \pm 3.7$ pcm, which can be considered during special situations as an initiation of prompt criticality. If the depressurization is followed by decrease of coolant temperature, the positive reactivity insertion will be compensated by the negative reactivity effect of the coolant temperature change.

3.1. Sensitivity Analysis

For the following evaluation and analyses the four most important reactivity effects were chosen from those presented in Table I and II. Reactivity effects of the fuel temperature change $\Delta T \approx \pm 800$ K represent the highest positive and negative possible reactivity insertion from the investigated cases and coolant void reactivity effect for coolant temperature 453 K and 913 K demonstrate temperature influence to the safety parameters. Main goal of this paper is to characterize selected reactivity effects using Perturbation Theory and utilize obtained results for preliminary optimization of most important reactivity effects. In the first step the sensitivity analysis of k_{eff} was carried out. The set of nuclides is mainly composed from the fuel isotopes (see Table III) but four structural nuclides were able to succeed to the ten most sensitive isotopes. Carbon and Rhenium can be partially assigned to the fuel due to their direct contribution to the fuel design functionality and integrity. Zirconium and Silicon are principal nuclides of reflector structure and their presence in the group of most sensitive nuclides demonstrates the weight of this structure in the core design.

TABLE III: SENSITIVITY COEFFICIENTS OF K_{EFF} FOR FISSILE AND FERTILE NUCLIDES.

Nuclide	Fission		Capture		Elastic scat.		Inelastic scat.	
	PORK	DP	PORK	DP	PORK	DP	PORK	DP
²³⁹ Pu	4.46E-01	4.40E-01	-4.40E-02	-4.34E-02	-1.95E-04	-1.92E-04	-4.44E-03	-4.81E-03
²⁴¹ Pu	8.61E-02	8.39E-02	-4.97E-03	-4.90E-03	-1.99E-05	-1.97E-05	-7.75E-04	-8.57E-04
²⁴⁰ Pu	4.31E-02	4.23E-02	-1.98E-02	-1.95E-02	-1.06E-04	-1.05E-04	-2.08E-03	-2.25E-03
²³⁵ U	2.70E-02	2.64E-02	-3.27E-03	-3.23E-03	-1.49E-05	-1.47E-05	-5.03E-04	-5.36E-04
²³⁸ U	8.90E-02	8.56E-02	-2.19E-01	-2.16E-01	-2.48E-03	-2.45E-03	-8.57E-02	-8.94E-02
²³⁸ Pu	1.36E-02	1.33E-02	-3.08E-03	-3.04E-03	-8.95E-05	-8.84E-06	-1.74E-04	-1.89E-04

Total sensitivity coefficients were validated by Direct Perturbation method (DP) for selected nuclides and reactions. Acceptable consistency was achieved for reactions fission, capture and elastic scattering of fuel isotopes. Difference between DP and sensitivity coefficients was less than 10 % what can be seen in Table III. The same level of consistency was achieved also for structural materials.

In the second step the sensitivity analysis of the reactivity effects for fuel temperature change was performed. The set of most sensitive nuclides was also defined and is nearly identical as it was for sensitivity of k_{eff} . In the group of nuclides of structural materials ⁹⁰Zr was replaced by ¹⁸⁵Re with relatively high sensitivity to capture. The sensitivity coefficients of Doppler reactivity effect for temperature change 1263 K → 2063 K and nuclides of structural materials are presented in Table IV. SCALE sensitivity coefficients for inelastic scattering were also compared but without serious validation effect. DP was carried out also for fissile and fertile nuclides where all calculated sensitivity coefficients were confirmed.

TABLE IV: SENSITIVITY COEFFICIENTS OF $\Delta\rho_{TFUEL}$ FOR NUCLIDES OF STRUCTURAL MATERIALS.

Nuclide	Capture		Elastic scat.		Inelastic scat.		
	PORK	DP	PORK	DP	PORK	DP	SCALE
C _{nat}	2.50E-05	2.49E-05	-9.48E-01	-8.34E-01	-3.89E-03	-4.04E-02	-1.98E-03
²⁸ Si	1.59E-03	1.58E-03	-1.16E-01	-1.32E-01	-2.79E-02	-2.96E-01	-3.48E-02
¹⁸⁷ Re	1.09E-01	1.09E-01	-9.09E-04	-1.11E-03	-7.81E-03	-7.93E-03	-7.37E-03
¹⁸⁵ Re	6.81E-02	6.79E-02	-4.73E-04	-6.33E-04	-4.57E-03	-4.65E-03	-4.16E-03

Sensitivity profiles of Doppler reactivity effect calculated by PORK and SCALE system are shown in FIG. 3. Overall profile match of fissile nuclides for fission and capture reactions was achieved. In some special cases the implicit part of sensitivity coefficient, which SCALE system is able to calculate, may result in deformation of the shape of the profile, compared to explicit part. This phenomenon is specific for sensitivities of k_{eff} and low energy groups, since the implicit part is included in both profiles which enter to sensitivity of reactivity effects calculations. Comparison of the profiles for inelastic scattering show similar shapes but different order of magnitude within some energy groups. Visual comparison confirmed the differences in integral sensitivity coefficients presented in Table IV for nuclides C_{nat} and ²⁸Si.

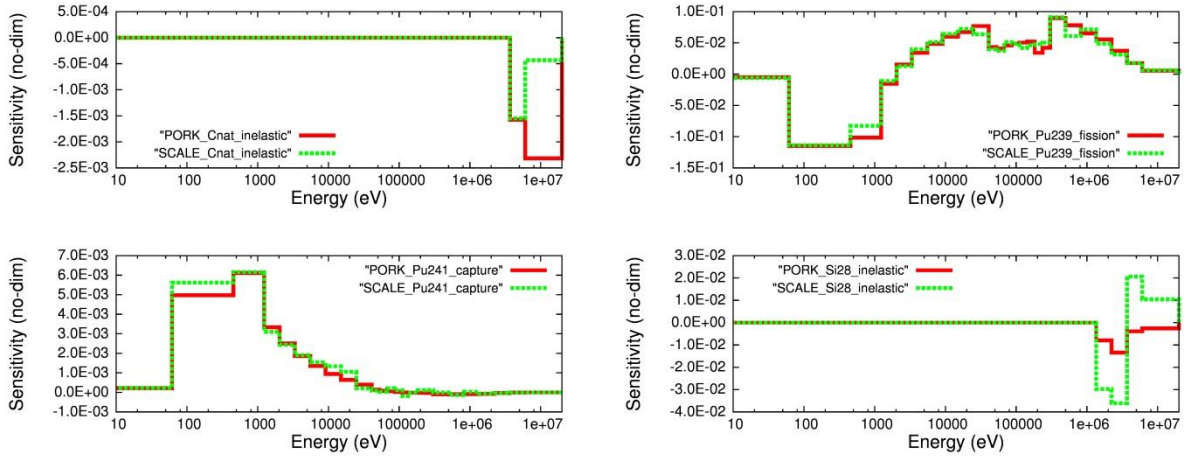


FIG. 3. Comparison of sensitivity profiles of Doppler reactivity effect for temperature change 1263 K \rightarrow 2063 K.

Last sensitivity analysis with DP validation was applied to the void reactivity effect. The validity of fissile and fertile nuclides sensitivity coefficients was confirmed by the DP calculation with standard accuracy. The group of structural materials was supplemented by ^4He (see Table V). Sensitivity coefficients of void reactivity effect with temperature 453 K of the coolant are presented in Table V. The inelastic scattering remained as problematic reaction for the same nuclides (C_{nat} , ^{28}Si , ^{90}Zr) in comparison with SCALE sensitivities.

TABLE V: SENSITIVITY COEFFICIENTS OF $\Delta\rho_{7\rightarrow 1}$ FOR NUCLIDES OF STRUCTURAL MATERIALS.

Nuclide	Capture		Elastic scat.		Inelastic scat.		
	PORK	DP	PORK	DP	PORK	DP	SCALE
^4He	0.00E+00	0.00E+00	1.19E+00	1.19E+00	0.00E+00	0.00E+00	0.00E+00
C_{nat}	9.52E-06	1.01E-05	-4.68E-01	-4.67E-01	-1.69E-04	-1.59E-04	-1.13E-03
^{28}Si	2.04E-03	1.92E-03	-1.39E-01	-1.39E-01	-2.35E-02	-2.33E-02	1.57E-02
^{90}Zr	1.21E-03	6.16E-04	-4.84E-02	-4.90E-02	-9.84E-04	-1.00E-03	3.27E-02
^{187}Re	6.12E-02	6.49E-02	-3.08E-04	-3.05E-04	-1.37E-02	-1.37E-02	-4.20E-03

Within sensitivity analysis the most important nuclides were identified from the perspective of selected reactivity effects and their subsequent modification. Despite the fact that the validation by DP was not fully successful for inelastic scattering, we can consider that the obtained results are acceptable for the present level of GFR 2400 development. In all investigated cases the dominance laid on fuel nuclides but the contribution of the reflector nuclides was not negligible, which demonstrates the importance of this structural part. At the same time, we cannot omit the Carbon and its impact, as the nuclide with one of the largest fraction in the core volume. The list of the most sensitive nuclides was very stable, what reduced the group of materials, which could influence selected reactivity effects. However, the identification of the suitable combination of ^{239}Pu , ^{238}U , ^{235}U , C and Si in combination with technological feasibility of proposed modification will not be an easy task.

3.2. Optimization of Reactivity Effects

The first goal was to find conservative design, which is not changing the reference design of GFR 2400 but it is employing the design features and amplifies their functionality. The design of GFR 2400 core offers a simple opportunity to place additional materials inside the core without any modification. Volume of the control and safety rod follower brings additional space for new materials influencing selected reactivity effects. The influence range of a material installed to the free volume of rod follower is questionable. Complex modifications, on the other side, include a change of the ratio of structural material of the core which could lead to a redesign of the core.

TABLE VI: REACTIVITY EFFECTS FOR PROPOSED CORE MODIFICATIONS.

Variant	$\Delta\rho_{7 \rightarrow 1}$ [pcm]		$\Delta\rho_{T_{fuel}}$ [pcm]	
	453 K	913 K	2063 K	453 K
Ref.	449.3 \pm 21.1	224.8 \pm 10.6	-503.7 \pm 14.3	1183.1 \pm 36.9
UC	463.8 \pm 22.3	233.9 \pm 11.2	-507.2 \pm 14.0	1227.8 \pm 36.8
C_full	399.3 \pm 21.9	200.3 \pm 11.0	-582.3 \pm 15.9	1305.6 \pm 40.6
^{235}U	362.0 \pm 20.8	180.6 \pm 10.4	-526.5 \pm 15.9	1238.2 \pm 41.3
C_full+ ^{235}U	334.0 \pm 18.3	167.6 \pm 9.2	-611.7 \pm 16.7	1356.3 \pm 42.2

The design of modified rod follower was based on the design of control and safety rod proposed in the paper [8], where the fundamental dimensions of wrapper tube, follower rod and other structural parts were defined. To fill rest of free volume, four materials were chosen based on the sensitivity analysis; UC, SiC, Zr_3Si_2 and C. In the case of UC, SiC and Zr_3Si_2 , pin type of arrangement was proposed and for C the completely filling of the free volume was used to maximize the moderation effect (denoted as C_full). The philosophy applied during material selection was to stay closest to the reactor design and minimize a usage of exotic materials. For correct definition of the UC during reactivity calculations, as a partially fissionable material, it was necessary to specify the appropriate operational temperature. The temperature of UC material was estimated from power of UC to power of surroundings fuel elements ratio. The results of selected reactivity effects for UC and C_full are presented in Table VI. The reactivity effects of UC, SiC and Zr_3Si_2 were very similar and therefore only results of UC are presented in this paper. Within conservative philosophy only C_full utilization brought the reasonable reactivity effects. More than 10 % improvement was achieved for both void reactivity effects. In the case of the fuel temperature reactivity effect for the temperature increase more negative value was obtained and for temperature decrease more positive value was achieved, which can be considered as a questionable improvement. It is better to have more negative temperature effect for situations of power rise but in process of shutting down or starting of reactor the core will be more resistant to these changes.

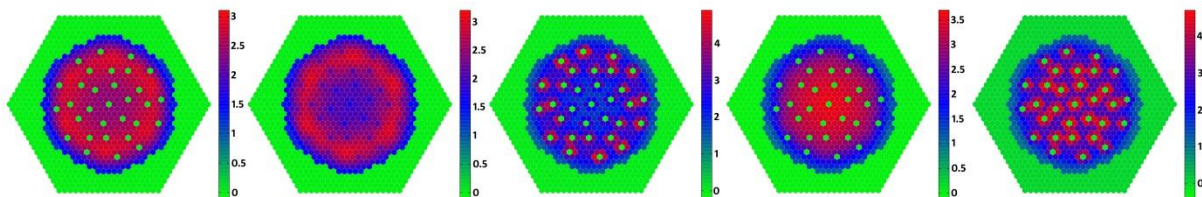


FIG. 4. Spatial distribution of Doppler reactivity effect for temperature change 1263 K \rightarrow 453 K (Ref., UC, C_full, ^{235}U , C_full+ ^{235}U).

Spatial distributions of the reactivity effects are presented in *FIG. 4* and *FIG. 5*. Utilization of the UC had mainly impact for Doppler reactivity effects in the center of the core (*see FIG. 4*). Absolute values were in both cases decreased, but comparable contribution of UC regions with the boundary areas compensated this effect. Similar behavior can be seen also for void reactivity effects but with lower influence in central region. Additional contribution of the UC in rod followers (change in parasitic absorption on U, *see FIG. 5*) therefore can explain the rise of integral reactivity effects. The filling of rod follower by Carbon multiplied the Doppler Effect in surrounding fuel elements which can be seen on the middle pictures of *FIG. 4* where the local maxima increased up to 50 %. In the case of void reactivity effects the influence of Carbon rod follower is more spread through the core. Reduction of the void effect can be seen in the central region of the core but with slight increase of maxima in outer part of the core (*see middle pictures of FIG. 5*).

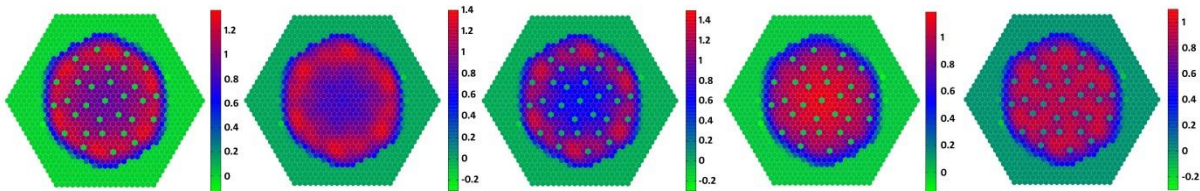


FIG. 5. Spatial distribution of void reactivity effect for pressure change 7 MPa \rightarrow 1 MPa and coolant temperature 453 K (Ref., UC, C_full, ^{235}U , C_full+ ^{235}U).

Based on the previous analysis and achieved results, new variants were investigated. Together they can be stated as complex modifications. Within this part of reactivity effects characterization, the control and safety rod rearrangement, several variations in the relative proportion of fuel assembly materials and isotopic composition of fuel material were investigated. The most valuable results were achieved by utilization of the low enriched Uranium where the mean enrichment by isotope ^{235}U was 5 %. Decrease of void reactivity effects was around 20 %, which in case with coolant temperature 453 K decreased the void effect below one β_{eff} . At the same time, the increase of the Doppler reactivity effect was not so important, which can be considered as required effect. The last variant was modeled as combination of the completely filled of free rod follower volume and usage of low enriched UC (C_full+ ^{235}U). This variant decreased the void reactivity effects to minimum but the growth of Doppler reactivity effect was also achieved. The results of the core design variants for complex modifications are presented in last two rows of Table VI.

In case of application enriched Uranium, entire change of spatial distribution of all reactivity effects can be seen. Spatial distribution of reactivity effects for reference design is characterized by the ring shape where the maximum values are located in the last ring of the control rods and toward to center and edge of core the absolute values of reactivity effect are decreasing. Combination of the enriched Uranium with Carbon rod follower resulted to two different spatial effects. In case of the Doppler reactivity effect additional moderation on Carbon supported the Doppler Effect in surrounding fuel elements and local maxima around control and safety rods was created, *see FIG. 4*. The effect of combination of these two modifications to void reactivity effect is again global. The ring shape of reference design or parabolic shape of U enriched design was flattened to a uniform distribution with small depressions around control and safety rods and boundary area, *see FIG. 5*.

4. Conclusion

The reactivity effects of the GFR 2400 core were calculated in range of pre-defined temperatures and coolant pressures. Coolant void reactivity effect for nominal and cold operational temperature and Doppler reactivity effects for the highest temperature increase and decrease were identified as the most important reactivity effects. Based on the sensitivity and uncertainty analysis for these reactivity effects, the most sensitive nuclides for optimization process were identified. The sensitivity coefficients were in the same time validated via direct perturbation calculation and energy profile comparison. Two ways of the core optimization were proposed, which were described as conservative and complex core modifications. Utilization of UC in the free rod follower volume did not demonstrated significant influence to the selected reactivity effects. Local effects and non-competitive moderation resulted to undesired increase of void reactivity effects. Better response was achieved by employment of the sole Carbon instead of UC. Moderation becomes competitive to Helium but only locally. Valuable improvement was obtained using enriched Uranium within complex modifications. Significant decrease of void reactivity effects with low modification of Doppler reactivity effects was one of the goals of the whole optimization process. Favorable response from application of Carbon and ^{235}U enrichment served as motivation for combination of these two design modifications which resulted to the best improvement of void reactivity effects. Increase of the Doppler reactivity effect for temperature change 1263→453 K about 170 pcm should be accepted as consequence of void reactivity effect reduction below one β_{eff} for coolant temperature 453 K.

Acknowledgment

This work was financially supported by grant of the Slovak Research and Development Agency No. APVV-0123-12.

References

- [1] M. Zabiego, et al., “Overview of CEA's R&D on GFR fuel element design: from challenges to solutions”, FR13, Paris, France, March 4-7, 2013
- [2] M. L. Williams, “Sensitivity and Uncertainty Analysis for Eigenvalue-Difference Responses”, Nuclear Science and Engineering, 155, pp. 18-36, 2007
- [3] Z. Perkó, et al., “Core Neutronics Characterization of the GFR2400 Gas Cooled Fast Reactor”, Progress in Nuclear Energy, 83, pp. 460–481, 2015.
- [4] B. M. Carmichael, “Standard Interface Files and Procedures for Reactor Physics Codes, Version III”, Report, LA-5486-MS, Los Alamos, 1974
- [5] K. L. Derstine, DIF3D 10.0, Argonne National Laboratory, Argonne, IL, 2011
- [6] D.H. Kim et al., “Validation Tests of the Multigroup Cross Section Libraries for Fast Reactors”, PHYSOR-2006, ANS Topical Meeting on Reactor Physics, Vancouver, Canada, 2006.
- [7] SCALE: A Comprehensive Modeling and Simulation Suite for Nuclear Safety Analysis and Design, ORNL/TM-2005/39, Version 6.1.3, Oak Ridge National Laboratory, Oak Ridge, Tennessee (2011).
- [8] Š. Čerba, et al., “Optimization of the heterogeneous GFR 2400 control rod design”, Progress in Nuclear Energy, *in press*.